Biochimica et Biophysica Acta 1804 (2010) 1500–1507

Contents lists available at ScienceDirect

Biochimica et Biophysica Acta

journal homepage: www.elsevier.com/locate/bbapap

Polyglutamine tract-binding protein-1 binds to U5-15kD via a continuous 23-residue segment of the C-terminal domain

Masaki Takahashi [a], Mineyuki Mizuguchi [a,*], Hiroyuki Shinoda [a], Tomoyasu Aizawa [b], Makoto Demura [b], Hitoshi Okazawa [c], Keiichi Kawano [b]

[a] Faculty of Pharmaceutical Sciences, University of Toyama, 2630, Sugitani, Toyama 930-0194, Japan
[b] Division of Biological Sciences, Graduate School of Science, Hokkaido University, Sapporo 060-0810, Japan
[c] Department of Neuropathology, Medical Research Institute, Tokyo Medical and Dental University, 1-5-45, Yushima, Bunkyo-ku, Tokyo 113-8510, Japan

ARTICLE INFO

Article history:
Received 30 November 2009
Received in revised form 11 March 2010
Accepted 13 March 2010
Available online 20 March 2010

Keywords:
Unstructured protein
Protein structure
PQBP-1
Polyglutamine
U5-15kD

ABSTRACT

Polyglutamine tract-binding protein-1 (PQBP-1) is a nuclear protein that interacts with various proteins, including RNA polymerase II and the spliceosomal protein U5-15kD. PQBP-1 is known to be associated with X-linked mental retardation in which a frameshift mutation in the *PQBP-1* gene occurs. In the present study, we demonstrate that PQBP-1 binds to U5-15kD via a continuous 23-residue segment within its C-terminal domain. Intriguingly, this segment is lost in the frameshift mutants of PQBP-1 associated with X-linked mental retardation. These findings suggest that the frameshift mutations in the *PQBP-1* gene lead to expression of mutants lacking the ability to interact with U5-15kD.

1. Introduction

Mental retardation (also called intellectual disability) is a developmental disability evident before age 18 years that is characterized by limitations in both intelligence and adaptive skills [1,2]. It is estimated that 1% to 3% of the world population is affected with mental retardation. Mental retardation can be caused by genetic as well as environmental factors that act on the development and functioning of the central nervous system prenatally, perinatally or postnatally [1,2]. Mental retardation is more frequent in males than in females, and thus mutations in genes on the X chromosome have long been considered to be important causes of mental retardation. The mental retardation which is caused by X-linked gene defects is called X-linked mental retardation (XLMR). According to the report by Chiurazzi et al. [1], there are at least eighty-two genes on the X chromosome that are associated with XLMR. Their gene products are related to regulation of transcription (22%), signal transduction (19%), regulation of the cell cycle and ubiquitin pathway (7%), DNA and RNA processing (6%), and so on.

The polyglutamine tract-binding protein-1 (PQBP-1) is one of the molecules involved in the pathology of XLMR [3,4]. PQBP-1 is a 265 amino acid protein that contains a WW domain, a polar amino acid-rich domain and a C-terminal domain [5,6] (Fig. 1). The *PQBP-1* gene is located on the X chromosome, and several mutations of the *PQBP-1* gene have been discovered in XLMR families [3,4]. For example, Kalscheuer et al. [3] discovered mutations in the *PQBP-1* gene in XLMR families referred to as N40 and N9/SHS. Lenski et al. [4] also reported *PQBP-1* mutations in other XLMR families referred to as K9008 and K8110. These mutations cause frameshifts that lead to premature stop codons, resulting in the expression of truncated PQBP-1 (Fig. 1).

In addition to XLMR, PQBP-1 is associated with polyglutamine disease pathology due to its direct interaction with polyglutamine-containing proteins such as huntingtin and ataxin-1 [5–7]. PQBP-1 is present in neurons throughout the brain, with abundant levels in the hippocampus, cerebellar cortex and olfactory bulb [5]. PQBP-1 is predominantly expressed in embryos and in newborn mice, and the expression level of PQBP-1 reaches a peak around birth and is down-regulated in adulthood [8]. Interestingly, PQBP-1-knockdown mice exhibit deficits in anxiety-related cognition and memory [9]. The knockdown leads to abnormal expression of memory-related genes that could be induced by dysfunction of PQBP-1 [9].

In the cell, PQBP-1 localizes to the nucleus and interacts with RNA polymerase II and U5-15kD, a component of the U5 small nuclear ribonucleoprotein particle (snRNP), which is one of the components of the spliceosome [7,10,11]. PQBP-1 interacts with RNA polymerase II via its WW domain [7] and with U5-15kD via its C-terminal domain

Abbreviations: hDim2, human Dim2; HSQC, heteronuclear single-quantum correlation; PQBP-1, polyglutamine tract-binding protein-1; PQBP-1-CT43, PQBP-1(223–265); snRNP, small nuclear ribonucleoprotein particle; XLMR, X-linked mental retardation

* Corresponding author.
E-mail address: mineyuki@pha.u-toyama.ac.jp (M. Mizuguchi).

1570-9639/$ – see front matter © 2010 Elsevier B.V. All rights reserved.
doi:10.1016/j.bbapap.2010.03.007

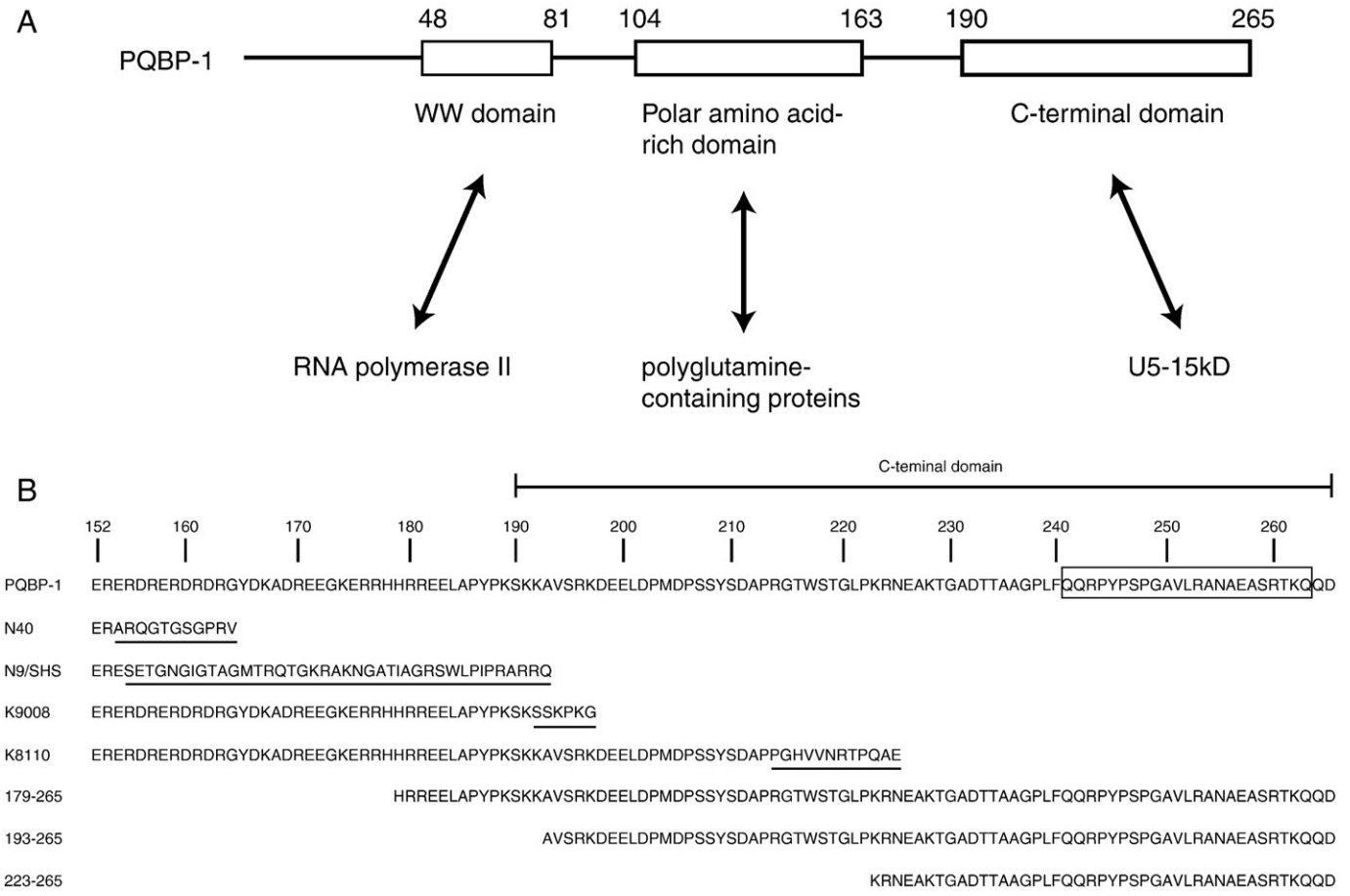

Fig. 1. (A) Domain structure of PQBP-1. PQBP-1 is a 265 amino acid protein that contains a WW domain, a polar amino acid-rich domain and a C-terminal domain [5,6]. The WW domain and the C-terminal domain interact with an RNA polymerase II and U5-15kD, respectively. The polar amino acid-rich domain interacts with polyglutamine-containing proteins such huntingtin and ataxin-1 [5,6]. (B) Partial amino acid sequences of wild-type PQBP-1 and its deletion mutants. N40, N9/SHS, K9008 and K8110 are the deletion mutants predicted by the open reading frame of PQBP-1-linked mental retardation patients. Amino acid changes due to frameshift mutations are underlined. The N-terminus-deletion mutants PQBP-1(179–265), PQBP-1(193–265) and PQBP-1(223–265) are designated as 179–265, 193–265 and 223–265, respectively. The position of the C-terminal domain is indicated above the sequences. The boxed amino acid sequence is the region required for the interaction with U5-15kD.

[10]. The interaction between PQBP-1 and RNA polymerase II is enhanced by phosphorylation of the second serine in a repeat sequence of the C-terminal domain of RNA polymerase II [7]. From these findings, PQBP-1 is considered a connector between transcription and splicing. However, it remains to be elucidated how the C-terminal domain of PQBP-1 interacts with the spliceosomal protein U5-15kD.

We have recently reported that PQBP-1 is composed of a large unstructured region and a small folded core [12]. The small folded core contains the WW domain, while the large unstructured region encompasses the polar amino acid-rich domain and the C-terminal domain. PQBP-1 includes a high content of unstructured regions in the C-terminal domain, even in the bound state with U5-15kD [12].

In this article, we focus on the interaction between the C-terminal domain and U5-15kD. We demonstrate that PQBP-1 binds to U5-15kD via a continuous 23-residue segment in its C-terminal domain, and that this segment is lost in the frameshift mutants of PQBP-1 associated with XLMR.

2. Materials and methods

2.1. Expression plasmids

A pGEX-6P-1 plasmid (GE Healthcare Bio-Sciences, Buckinghamshire, UK) for expression of full-length PQBP-1 (residues 1–265) was described previously [12]. The cDNA of the truncated PQBP-1 was subcloned into pGEX-6P-1 predigested with BamHI and SalI (GE Healthcare Bio-Sciences). The cDNA of U5-15kD was inserted between the NdeI and XhoI sites of pET22b(+) (Novagen, Madison, WI). We performed site-directed mutagenesis using a QuikChange™ site-directed mutagenesis kit from Stratagene (La Jolla, CA). We checked the sequence of the inserted DNA using an ABI PRISM 3100 Genetic Analyzer (Applied Biosystems, Foster City, CA).

2.2. Expression and purification of recombinant proteins

PQPB-1 and its truncated mutants were expressed as a GST-fusion protein. U5-15kD was expressed as a histidine-tagged protein: U5-15kD has six consecutive histidines at the C-terminus. All proteins were expressed in *Escherichia coli* strain BL21(DE3) with LB medium or C.H.L. medium (Chlorella Industry, Tokyo, Japan). Protein expression was induced by the addition of isopropyl-β-D-thiogalactopyranoside at a final concentration of 1 mM. After a 4-hour incubation at 31 °C, the cells were harvested by centrifugation. Cell pellets from 1-liter cultures were resuspended in 50 mL of 50 mM sodium phosphate and 2 mM dithiothreitol (pH 7.6). The cells were disrupted by sonication on ice with a probe-type sonicator (Branson sonifier 250; Branson Ultrasonics, Danbury, CT). All proteins were detected in a soluble fraction after centrifugation at 5000 rpm for 20 min at 4 °C.

GST-fusion proteins were purified with glutathione Sepharose 4B (GE Healthcare Bio-Sciences). The purified fusion protein was then

digested with PreScission protease (GE Healthcare Bio-Sciences) for 16 h at 5 °C to remove the GST region, and then the digested fusion protein was loaded onto a PD-10 column. The elution from the PD-10 column was passed through DEAE Sepharose Fast Flow (GE Healthcare Bio-Sciences), and the flow-through fractions were collected. The purified samples of the truncated PQBP-1 have an N-terminal (Gly-Pro-Leu-Gly-Ser) extension derived from the expression plasmid.

The cell lysate including U5-15kD was applied onto a Ni-NTA agarose column equilibrated with 50 mM phosphate buffer containing 0.3 M NaCl and 2 mM dithiothreitol (pH 7.6). The proteins were further purified by gel-filtration on a Superdex 75 column (GE Healthcare Bio-Sciences) equilibrated with 50 mM phosphate, 0.3 M NaCl and 10 mM 2-mercaptoethanol (pH 7.4). We used U5-15kD(1–128), the U5-15kD protein lacking the C-terminal 14 amino acids, because the full-length U5-15kD has autocleavage activity. Its autocleavage results in U5-15kD(1–128) or (1–129) due to the cleavage at positions 128 or 129 [11,13,14].

2.3. GST pull-down assay

The binding activity of PQBP-1 was analyzed by a GST pull-down assay. Glutathione Sepharose beads were mixed and precipitated with GST or GST-PQBP-1. The GST protein expressed by an empty pGEX-6P-1 vector was used as a negative control. After incubation for 60 min at 4 °C, the beads were washed three times with 50 mM phosphate buffer containing 2 mM dithiothreitol (pH 7.6). The beads were mixed with U5-15kD solutions and incubated for 60 min at 4 °C. The beads were then washed three times with the phosphate buffer and mixed with SDS-PAGE sample buffer. The bound proteins were analyzed by SDS-PAGE and stained with Coomassie Brilliant Blue. The intensity of each band was quantified using ImageJ software (available at http://rsbweb.nih.gov/ij/). The binding activity of the GST-fusion protein was given by the intensity ratio of U5-15kD to GST-fusion protein.

2.4. NMR spectroscopy

Isotopically labeled proteins were overexpressed in C.H.L. medium (Chlorella Industry) or M9 medium supplemented with [^{15}N]NH_4Cl and [^{13}C]glucose as the sole nitrogen and carbon sources. NMR samples were prepared in 10 mM sodium phosphate, 0.1 mM EDTA, 50 μM 2,2-dimethyl-2-silapentane-5-sulfonate sodium salt and 5% D_2O (pH 7.5). The protein concentration was 0.3–0.4 mM. For backbone assignments of PQBP-1(223–265) and U5-15kD, ^{15}N/^{13}C-labeled samples were prepared for the CBCANH/CBCA(CO)NH and HN(CA)CO/HNCO experiments. All NMR experiments were performed on a Bruker DMX500 spectrometer (Bruker BioSpin, Rheinstetten, Germany). NMR data were processed with NMRPipe [15] and analyzed with NMRView [16].

For titration experiments, a series of samples were prepared in which the U5-15kD:PQBP-1(223–265) molar ratios ranged from 1:0 to 1:3.9. A ^{1}H–^{15}N heteronuclear single-quantum correlation (HSQC) spectrum of U5-15kD was recorded at each titration point. The chemical shift perturbation ($\Delta\delta$) was calculated by the equation,

$$\Delta\delta = \sqrt{(0.17\Delta^{15}N)^2 + (\Delta^1H)^2}, \quad (1)$$

in which Δ^{15}N represents the change in the chemical shift of the amide nitrogen and Δ^1H represents the change in the chemical shift of the amide proton [17].

We obtained the dissociation constant, K_d, assuming a 1:1 binding model. In this model, $\Delta\delta$ is represented by

$$\Delta\delta = \frac{\Delta\delta_{max}}{2P_1}\left\{(P_1 + P_2 + K_d) - \sqrt{(P_1 + P_2 + K_d)^2 - 4P_1P_2}\right\}. \quad (2)$$

In Eq. (2), $\Delta\delta_{max}$ is the chemical shift change between the free and bound forms, and P_1 and P_2 are the total concentrations of U5-15kD and PQPB-1-CT43, respectively. We analyzed the titration curves on the basis of Eq. (2) using the non-linear least-squares method. In the analysis, we performed a global fitting, in which the titration curves for different residues were fitted simultaneously, on the assumption that the K_d is common for all residues.

3. Results

3.1. Binding activity of deletion mutants of PQBP-1 to U5-15kD

It has been reported that the frameshift mutations in the *PQBP-1* gene are associated with XLMR [3,4]. However, little is known about the effects of the frameshift mutations on the binding activities of PQBP-1 to U5-15kD. We examined the binding activities of N40, N9/SHS, K9008 and K8110, all of which are caused by a frameshift mutation in the *PQBP-1* gene (Fig. 1). These frameshift mutations result in amino acid changes and premature stop codons, which lead to the truncations of PQBP-1 (Fig. 1). The truncations caused by the mutations act on the C-terminal domain, which is indispensable for interaction with U5-15kD [10]. We examined the binding activities using a GST pull-down assay, and the results appeared to show that the binding activities of the frameshift mutants are strongly reduced (Fig. 2).

We also examined which part of the C-terminal domain is sufficient for the interaction with U5-15kD using a series of N-terminal deletion mutants. The N-terminal deletion mutants used were PQBP-1(179–265), PQBP-1(193–265) and PQBP-1(223–265). Fig. 2 shows that all of the deletion mutants bound to U5-15kD, and thus the residues 223 to 265 of PQBP-1 appear to be sufficient for the interaction with U5-15kD. The fragment PQBP-1(223–265) is called PQBP-1-CT43 in the following.

3.2. Titration of PQBP-1-CT43 to ^{15}N-labeled U5-15kD

The full-length PQBP-1 and U5-15kD have molecular weights of 30 kDa and 17 kDa, respectively, and thus the complex of PQBP-1 and U5-15kD is too large to be detected directly by NMR spectroscopy. We

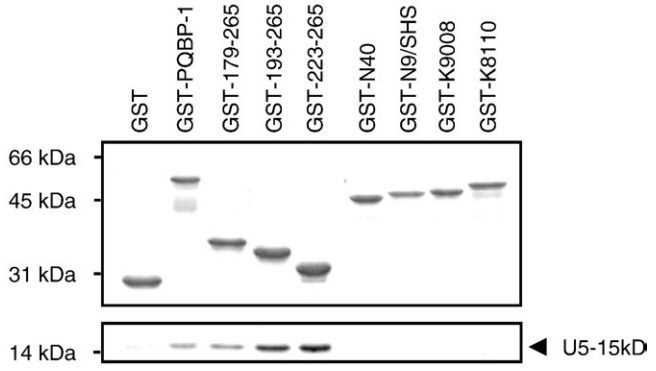

Fig. 2. Analysis of the interactions between PQBP-1 mutants and U5-15kD. The interactions are analyzed by a GST pull-down assay. U5-15kD was mixed with GST or GST-fusion protein of the PQBP-1 mutants. Proteins bound to glutathione Sepharose beads were analyzed by SDS-PAGE and stained with Coomassie Brilliant Blue. GST-179–265, GST-193–265 and GST-223–265 are GST-fusion proteins of PQBP-1(179–265), PQBP-1(193–265) and PQBP-1(223–265), respectively. GST-N40, GST-N9/SHS, GST-K9008 and GST-K8110 are GST-fusion proteins of the frameshift mutants of PQBP-1 associated with XLMR [3,4].

therefore used PQBP-1-CT43 to study the interaction between PQBP-1 and U5-15kD.

In order to study the interaction at the amino acid level, the backbone resonances of U5-15kD were assigned sequence specifically (Fig. S1). The ^{1}H–^{15}N HSQC spectrum of ^{15}N-labeled U5-15kD was well-resolved, consistent with the rigid globular structure of U5-15kD [18]. To probe the interaction between PQBP-1-CT43 and U5-15kD, we recorded the ^{1}H–^{15}N HSQC spectra of ^{15}N-labeled U5-15kD titrated with unlabeled PQBP-1-CT43. Fig. 3A and B shows the ^{1}H–^{15}N HSQC spectra of ^{15}N-labeled U5-15kD in the presence of PQBP-1-CT43 at the molar ratios of 0.4 and 1.0 (PQBP-1-CT43/U5-15kD), respectively. The titration experiments indicated that the binding of PQBP-1-CT43 causes signal attenuation as well as chemical shift changes (Fig. 3A and B).

We examined two types of attenuation in the HSQC of ^{15}N-labeled U5-15kD titrated with PQBP-1-CT43 (Fig. 4).

One was the global attenuation. For example, the signal intensity was globally reduced to less than 80% of the free state over the whole sequence at the molar ratio of 0.4 (PQBP-1-CT43/U5-15kD) (Fig. 4A). The global attenuation was more prominent at the molar ratio of 1.0

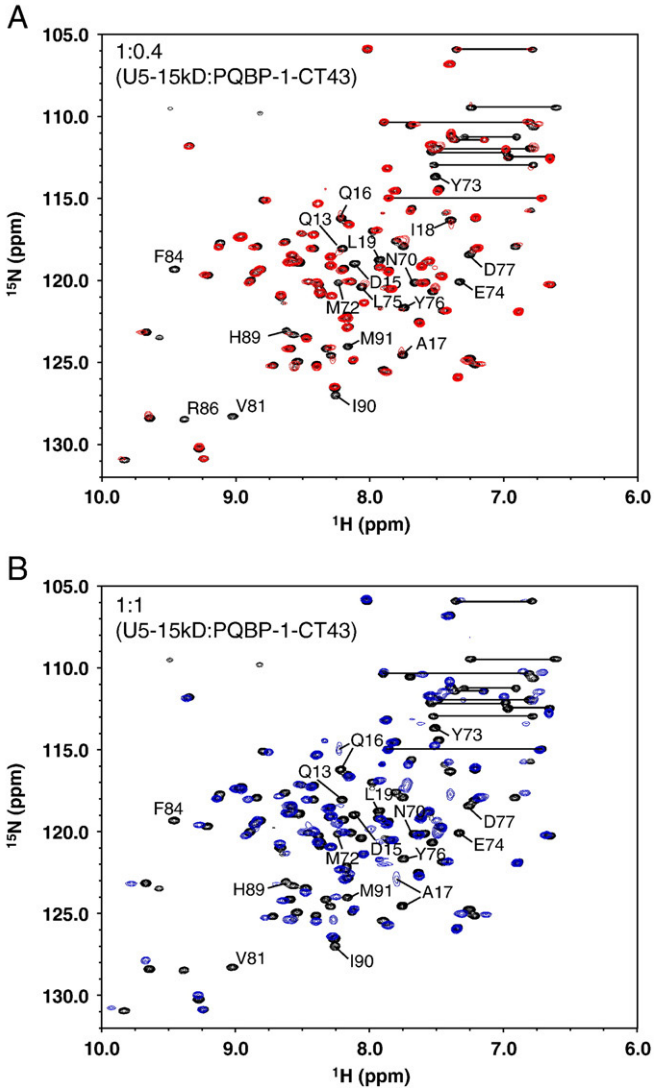

Fig. 3. ^{1}H–^{15}N HSQC spectra of ^{15}N-labeled U5-15kD titrated with PQBP-1-CT43 (red or blue contour). The molar ratios (U5-15kD:PQBP-1-CT43) were 1:0.4 (A) and 1:1 (B). The HSQC spectrum of the free U5-15kD is shown for comparison (black contour). The spectra were recorded at 37 °C. (A) Residues with intensity ratios (I_{bound}/I_{free})<0.2 are labeled. (B) Residues with intensity ratios (I_{bound}/I_{free})<0.1 are labeled.

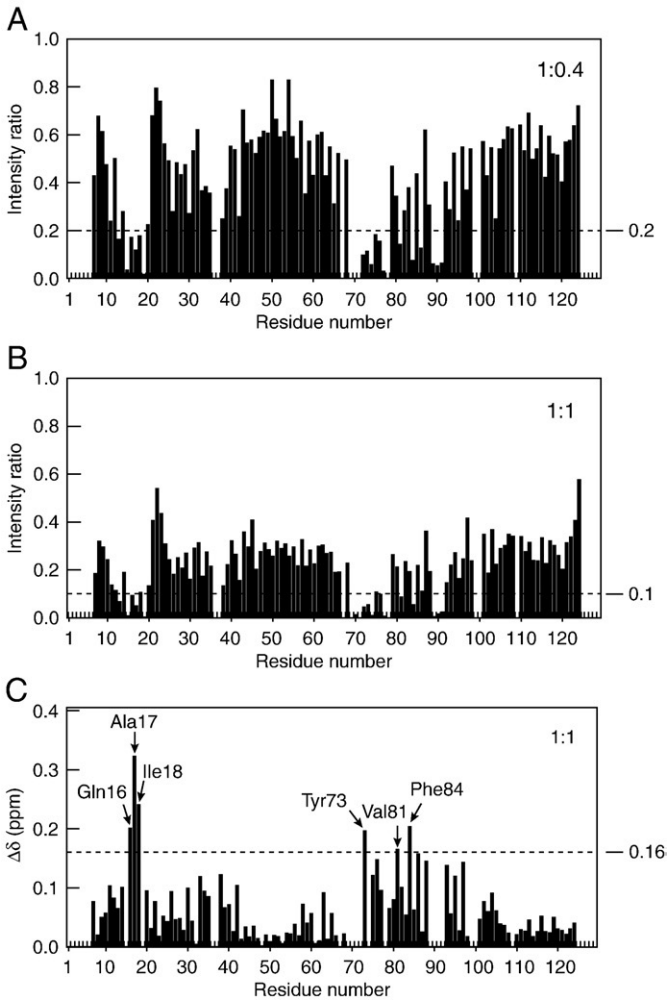

Fig. 4. Peak intensity changes (A and B) and chemical shift perturbations (C) of U5-15kD following the interaction with PQBP-1-CT43. The molar ratios (U5-15kD:PQBP-1-CT43) were 1:0.4 (A) and 1:1 (B and C). Missing and overlapping residues (Met1, Ser2, Tyr3, Met4, Leu5, Pro6, Pro36, Thr37, Pro67, Phe69, Lys71, Pro78, Asn99, Asn100, Lys109, Lys125, Gly126, Arg127 and Gly128) were eliminated from the analysis. The perturbation cut-off values are shown by dashed lines. (A and B) The intensity ratios (I_{bound}/I_{free}) for each residue were plotted against the residue number. (C) Chemical shift deviations ($\Delta\delta$) were calculated by $[(\Delta H)^2+(0.17\Delta N)^2]^{1/2}$. Gln16, Ala17, Ile18, Tyr73, Val81 and Phe84 are indicated by arrows.

(Fig. 4B); the signal intensity was globally reduced to less than 60% of the free state over the whole sequence. The global attenuation results from an increase in the overall correlation time [19], which is sensitive to the Stokes radius of the protein. The C-terminal domain is unstructured [12], and thus the binding of the elongated PQBP-1-CT43 results in a much larger Stokes radius [19,20].

The other type was the differential attenuation; that is, the attenuation of the signal intensity was stronger than the global attenuation [19,21]. The differential attenuation results from a dynamic interaction between two proteins on an intermediate/slow time scale (μs–ms) with respect to the NMR chemical exchange [19,22]. We utilized the differential attenuation to investigate the interaction sites between PQBP-1-CT43 and U5-15kD. When the molar ratio is 0.4 (PQBP-1-CT43/U5-15kD), several backbone resonances were reduced to less than 20% of the free state (Fig. 4A). A differential attenuation was also identified at the molar ratio of 1.0: several resonances were reduced to less than 10% of the free state (Fig. 4B). The attenuated resonances upon binding of PQBP-1-CT43 originate from residues in the α1 helix, the loop β2–β3, the strand β3, the loop β3–β4, and the strand β4 (Fig. 5A). These residues are located on one face of U5-15kD (Fig. 5B).

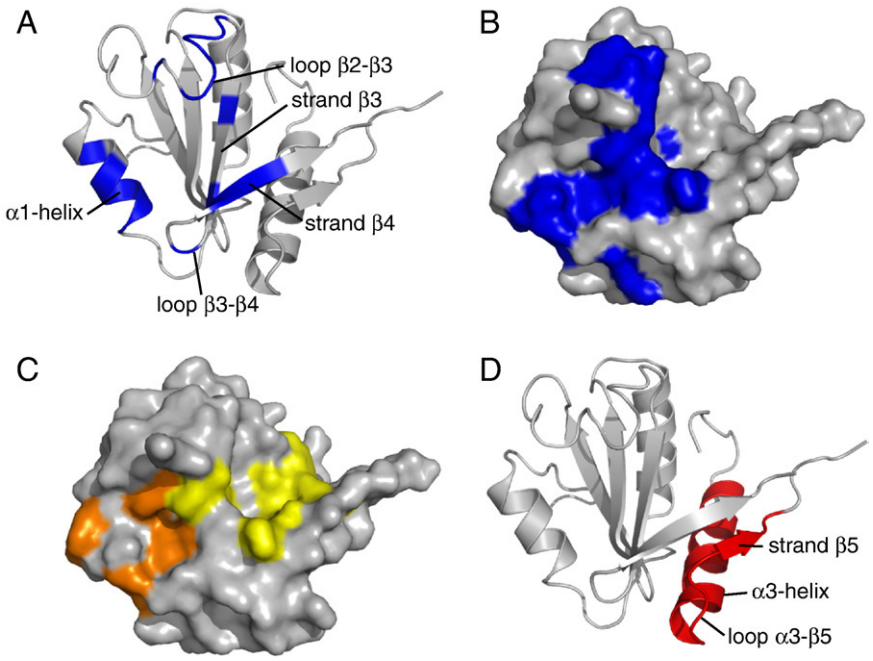

Fig. 5. Ribbon (A and D) and surface (B and C) representation of U5-15kD (PDB: 1QGV). U5-15kD has a thioredoxin-like fold, which is characterized by a four-stranded β-sheet consisting of pairs of parallel and antiparallel strands flanked by three α-helices. (A and B) Residues with strong signal attenuation upon binding to PQBP-1-CT43 are colored blue: the colored residues have an intensity ratio <0.2 at 1:0.4 (U5-15kD:PQBP-1-CT43) and/or a ratio <0.1 at 1:1. The α1 helix contains Gln13, Asp15, Gln16, Ala17, Ile18 and Leu19. The loop β2–β3 contains Asn70, Met72, Tyr73, Glu74, Leu75, Tyr76 and Asp77. The strand β3 contains Val81 and Phe84. The loop β3–β4 contains Arg86. The strand β4 contains His89, Ile90 and Met91. (C) The hydrophobic cleft and the hydrophobic groove are colored yellow and orange, respectively. (D) The Glu111–Ser132 are colored red. U5-15kD binds to a GYF domain of U5-52K via the residues from Glu111–Ser132.

In addition to signal attenuation, the addition of PQBP-1-CT43 caused chemical shift changes in the ^{1}H–^{15}N HSQC of U5-15kD (Fig. 4C). The chemical shift changes were clearly observed when the molar ratio was more than 1. The residues with large chemical shift changes are Gln16, Ala17, Ile18, Tyr73, Val81, and Phe84 (Fig. 4C). These residues are included in the PQBP-1-binding sites, which are identified by the differential attenuation (Fig. 5). At the molar ratio of 0.4 (PQBP-1-CT43/U5-15kD), the chemical shift changes were small, while several resonances were strongly attenuated (Fig. 3A).

For some well-resolved peaks, $\Delta\delta$ values were plotted as a function of the molar ratio of PQBP-1-CT43 and U5-15kD (Fig. S2). The plots were fitted globally to a 1:1 binding model using Eq. (2) (see Materials and methods). This analysis shows that the binding of PQBP-1-CT43 and U5-15kD can be described by the 1:1 binding model and that the dissociation constant (K_d) is 56 ± 8 μM.

3.3. PQBP-1 binds to U5-15kD via its 23-residue C-terminal segment

In order to further study the interaction between PQBP-1 and U5-15kD, we utilized the ^{1}H–^{15}N HSQC spectra of PQBP-1-CT43. Fig. 6A and B shows the ^{1}H–^{15}N HSQC spectra of ^{15}N-labeled PQBP-1-CT43 in the absence and presence of U5-15kD. The HSQC spectrum of PQBP-1-CT43 in the free form is typical of an unstructured protein (Fig. 6A), since the backbone resonances are clustered together in a limited frequency range, spanning less than 0.7 ppm in the ^{1}H dimension [23]. We made backbone resonance assignments for all residues of PQBP-1-CT43 except for Gly(-5) at the N-terminus (Fig. S3).

As in the HSQC spectrum of U5-15kD, there were also two types of attenuation in the HSQC spectrum of PQBP-1-CT43 titrated with U5-15kD (Fig. 6C). The signal intensity was globally reduced to less than 30% of the free state over the whole sequence. In addition to the global attenuation, the resonances from the residues 241 to 263 were strongly attenuated upon binding to U5-15kD (Fig. 6C). From this, we conclude that PQBP-1 binds to U5-15kD via a single continuous segment composed of 23 residues within the C-terminal domain. In addition to signal attenuation, the HSQC of PQBP-1-CT43 showed two new peaks separated from the majority of other peaks upon binding to U5-15kD (Fig. 6B). These new peaks originate from the continuous segment in the bound state with U5-15kD, and indicate a small number of residues being fixed due to the interaction with U5-15kD. Furthermore, these peaks were weaker than the other observable peaks. This appears to be consistent with the fact that a small number of residues become less mobile than the remainder of the protein following the binding to U5-15kD.

3.4. Critical residues for the interaction with U5-15kD

To explore the contribution of individual side chains in the C-terminal segment to the binding activity of PQBP-1-CT43, we applied alanine scanning mutagenesis to the region comprising residues 241-264 (Fig. 7). The binding activity was analyzed by a GST pull-down assay (Fig. S4). We performed a quantitative densitometric analysis of band intensities in the stained gels. The intensity ratio of U5-15kD to GST-fusion protein was calculated as a measure of the activity of GST-PQBP-1-CT43 and its mutants. This experiment was performed independently three times, and the mean values and standard deviations are shown in Fig. 7. We performed a *t*-test to assess whether the binding activity of the mutant was significantly different from wild-type. Differences at *P*-values <0.05 were considered significant.

The alanine substitutions markedly reduced the binding activity in the case of Y245A, V251A and L252A (Fig. 7). On the other hand, the N255A and R260A mutations slightly reduced the binding activity, although the effect of R260A was very small. We also generated a double point mutant (Y245A/N255A), which showed a strongly reduced binding activity of PQBP-1-CT43. The effect of the double mutation was greater than the effects of the single point mutations (Y245A or N255A).

In addition to the alanine mutagenesis, we examined Y245F and N255D mutations (Fig. 7). The Y245F mutation reduced the binding

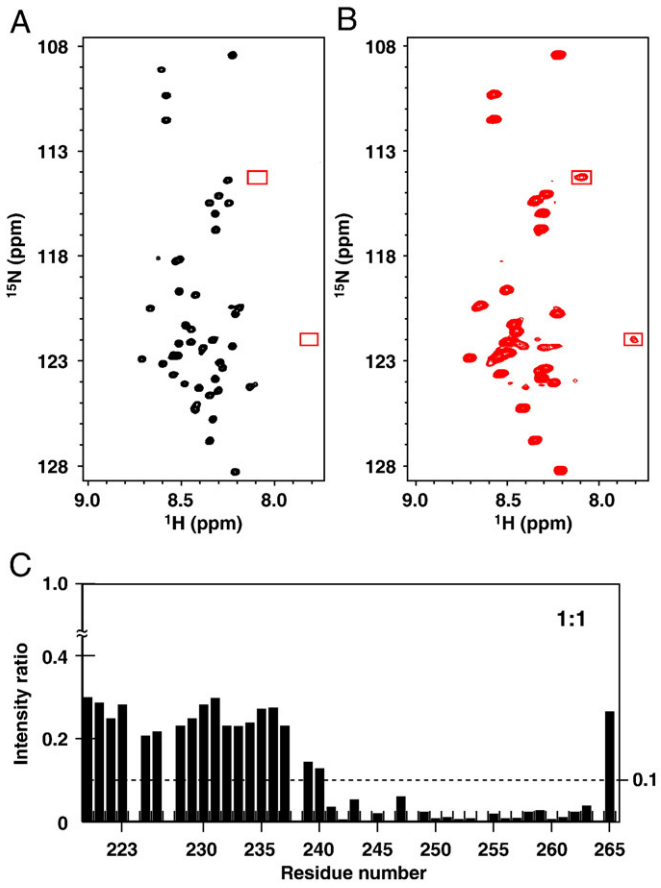

Fig. 6. (A, B) ^{1}H–^{15}N HSQC spectra of ^{15}N-labeled PQBP-1-CT43 in the absence (A) and presence (B) of U5-15kD. The positions of the new resonances which appear in the bound state are indicated by boxes. The spectra were recorded at 15 °C. (B) The molar ratio (PQBP-1-CT43:U5-15kD) was 1:1. (C) Peak intensity changes of PQBP-1-CT43 following the interaction with U5-15kD. The intensity ratios (I_{bound}/I_{free}) for each residue were plotted against the residue number. Overlapping residues (Arg224, Ala227, Ala254 and Gln264) were eliminated from the analysis. The perturbation cut-off value is indicated by a dashed line. The molar ratio (PQBP-1-CT43:U5-15kD) was 1:1.

activity, and thus a hydroxyl group of Tyr245 contributes to the interaction. The phenyl group of Tyr245 also contributes to the binding activity, since the binding activity of Y245F was slightly

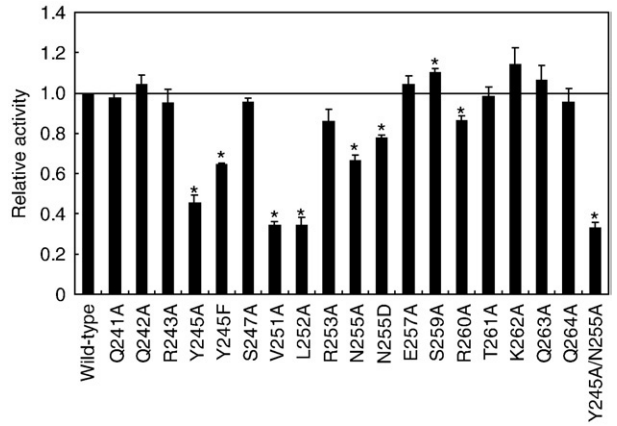

Fig. 7. Relative binding activity of PQBP-1-CT43 and its mutants with U5-15kD. The binding activity was analyzed by a GST pull-down assay. PQBP-1-CT43 and its single or double point mutants were examined. The GST pull-down assay was performed independently three times. The binding activity was normalized to the wild-type. The data represent mean values ± standard deviation from three independent assays. Asterisks indicate significant difference compared with wild-type (*t*-test, $P<0.05$).

higher than that of Y245A. The N255D mutation gave rise to a similar conclusion: the amino group of Asn255 contributes to the interaction, since the N255D mutation reduced the binding activity.

4. Discussion

Many proteins or regions of proteins are unstructured in their native, functional state. These proteins are referred to as "intrinsically unstructured" or "intrinsically disordered" [24–26]. Intrinsically unstructured proteins carry out important functions in key biological processes, such as regulation of transcription and signal transduction [24–27]. It is known that the prevalence of intrinsically unstructured proteins increases as the complexity of the organism increases [25]. For example, 2.0% of archaean, 4.2% of eubacterial and 33.0% of eukaryotic proteins are predicted to have long unstructured segments (>30 consecutive residues) in their native, functional state [28]. The high prevalence of intrinsically unstructured proteins in complex organisms implies that the lack of an ordered structure confers advantages in terms of protein function [29].

Many intrinsically unstructured proteins function by molecular recognition via binding to the target molecule [24,25]. Upon binding to the target, the unstructured regions often undergo coupled folding and binding [24,30]. However, there are several studies that show that unstructured proteins remain disordered even in the bound state [27,29,31,32]. These persistently unstructured proteins would appear to constitute a new category of intrinsically unstructured proteins.

The binding of U5-15kD results in strong attenuation of the resonances originating from residues 241 to 263 of PQBP-1-CT43. From this, we conclude that the binding site is a continuous segment of residues 241–263 within the C-terminal domain, and that this segment undergoes some conformational and dynamical changes upon binding to U5-15kD. In addition, the binding to U5-15kD gave rise to a small number of new peaks in the HSQC spectrum of PQBP-1-CT43. This implies that the binding is driven by a small number of residues in the C-terminal domain. The critical residues for the binding may become less mobile than the remainder of the C-terminal domain following binding to U5-15kD, because the new peaks were weaker than other observable peaks [31]. On the other hand, there was no significant chemical shift change in residues 193–240 of PQBP-1 following the binding to U5-15kD [12]. This means that the residues 193–240, that is, the C-terminal domain except for the binding segment, remains unstructured even in the bound state. This unstructured region may act as a spacer between RNA polymerase II and a spliceosome, when PQBP-1 connects these large multiprotein complexes [12].

Our present results demonstrate that the segment needed for the U5-15kD-binding is lost in N40, N9/SHS, K9008, and K8110 [3,4]. These findings suggest that the frameshift mutations in the *PQBP-1* gene lead to expression of mutants lacking the ability to interact with U5-15kD. To test this hypothesis, we examined the binding activity of the mutants (N40, N9/SHS, K9008, and K8110) using a GST pull-down assay. Our results appear to show that these frameshift mutations cause the loss of binding to U5-15kD.

Reuter et al. [18] revealed that U5-15kD possesses two hydrophobic areas on one face of the molecule. One is called the hydrophobic cleft, which is comprised of solvent-exposed hydrophobic residues Met72, Met82, Met91, Ile92, Leu94, Ile102, and Trp104 (Fig. 5C). The other one is the hydrophobic groove comprising residues Trp12, Val14, Ile18, Leu19, Phe30, Phe69 and Phe84 (Fig. 5C). These hydrophobic areas are surrounded by the positively and negatively charged residues [18].

The hydrophobic areas discussed above partially overlap with the PQBP-1-binding surface on U5-15kD (Fig. 5B and C). This is consistent with the fact that the hydrophobic residues V251 and L252 of PQBP-1 are critical for the interaction with U5-15kD. However, it does not mean that the polar interaction is not important for the interaction. Mutational analysis indicates that the hydroxyl group of Tyr245 and

the amino group of Asn255 in PQBP-1 are involved in the interaction between PQBP-1 and U5-15kD. In support of this view, the binding of PQBP-1 to U5-15kD was inhibited in the presence of high salt concentrations (Fig. S5).

In general, protein–protein interactions are energetically driven by only a small subset of residues, called "hot spots," localized at the contact interface [22,33], although protein–protein interactions are believed to originate from large contact surfaces involving 10–30 side chains from each protein component [22,34]. The residues Y245, V251 and L252 of PQBP-1 probably correspond to the hot spot for the interaction with U5-15kD.

It is known that U5-15kD interacts with other spliceosomal proteins, in addition to PQBP-1. One of the proteins is U5-52K, which is one component of the U5 snRNP [35]. U5-52K is recruited to the U5 snRNP, but dissociates from the U5 snRNP during the assembly of U5 and U4/U6 snRNP [36].

U5-52K simultaneously binds to U5-15kD and U5-102K, both of which are present in the U5 snRNP [36]. While U5-102K interacts with the N-terminal two-thirds of U5-52K, the interaction between U5-52K and U5-15kD is mediated by a C-terminal GYF domain of U5-52K and the Glu111–Ser132 of U5-15kD [35,36]. The Glu111–Ser132 of U5-15kD contains the α3 helix, the loop α3–β5, and the strand β5 (Fig. 5D). Based on the chemical properties of the side chains at the interaction surface, this interaction is dominated by polar interactions [35]. Keeping this in mind, we next considered the interaction between PQBP-1 and U5-15kD. The interaction surface of U5-15kD for the PQBP-1-binding is different from that for the U5-52K-binding: the PQBP-1-binding site resides within the α1 helix, the loop β2–β3, the strand β3, the loop β3–β4, and the strand β4. Furthermore, the binding is driven by both hydrophobic and polar interactions. Taken together, these findings suggest that the two separated protein-binding sites enable U5-15kD to play two distinct functions. U5-15kD, U5-52K and U5-102K exist simultaneously in the U5-snRNP [36]. On the other hand, U5-15kD, U5-102K and PQBP-1 are found in the complex of U2, U4, U5 and U6 snRNP [37]. RNA processing involving PQBP-1 and U5-15kD may be affected by polyglutamine-containing proteins such as huntingtin and ataxin-1, since PQBP-1 binds to expanded polyglutamine tracts via its polar amino acid-rich domain [5,6].

While U5-15kD interacts with PQBP-1, its homologous protein Dim2 cannot interact with PQBP-1 [38]. U5-15kD shares 38% sequence identity and 65% sequence similarity with human Dim2 (hDim2) [38]. U5-15kD is also called human Dim1, and is a human ortholog of fission yeast Dim1, which was first reported as an essential protein for entry into mitosis as well as for chromosome segregation during mitosis [39].

Comparison of the structures of hDim2 and U5-15kD reveals that the structure of hDim2 contains an extra α-helix and a β-strand [40]. In addition to the secondary structure difference, their quaternary structures are quite different: U5-15kD is a monomer while hDim2 is a dimer [40]. Although both U5-15kD and hDim2 are involved in pre-mRNA splicing and the control of cell cycle progression, these proteins seem to have different biological functions. For example, U5-15kD binds to PQBP-1 while hDim2 does not, as discussed above [38]. Why do these homologs carry out different functions, although U5-15kD and hDim2 share a common thioredoxin-like fold? The dimer structure of hDim2 revealed that the monomer–monomer interface is formed mainly by the α1 and α3 helices, the loop β3–β4 and the loop α4–β6 [40]. This monomer–monomer interface includes Tyr69 and Tyr72, which are crucial residues for the dimer formation [40]. The Tyr69 and Tyr72 of hDim2 correspond to Phe69 and Met72 of U5-15kD, which are located on the interaction surface with PQBP-1. This means that the PQBP-1 binding surface on the hDim2 monomer is blocked by another monomer. In light of these observations, we conclude that hDim2 cannot interact with PQBP-1 because the PQBP-1 binding surface is not solvent-exposed in the dimeric hDim2.

Acknowledgements

This study was supported by Grants-in-Aid for Scientific Research on Innovative Areas (Research in a Proposed Research Area) from the Ministry of Education, Culture, Science and Technology of Japan.

Appendix A. Supplementary data

Supplementary data associated with this article can be found, in the online version, at doi:10.1016/j.bbapap.2010.03.007.

References

[1] P. Chiurazzi, C.E. Schwartz, J. Gecz, G. Neri, XLMR genes: update 2007, Eur. J. Hum. Genet. 16 (2008) 422–434.
[2] H.H. Ropers, B.C. Hamel, X-linked mental retardation, Nat. Rev. Genet. 6 (2005) 46–57.
[3] V.M. Kalscheuer, K. Freude, L. Musante, L.R. Jensen, H.G. Yntema, J. Gécz, A. Sefiani, K. Hoffmann, B. Moser, S. Haas, U. Gurok, S. Haesler, B. Aranda, A. Nshedjan, A. Tzschach, N. Hartmann, T.C. Roloff, S. Shoichet, O. Hagens, J. Tao, H. Van Bokhoven, G. Turner, J. Chelly, C. Moraine, J.P. Fryns, U. Nuber, M. Hoeltzenbein, C. Scharff, H. Scherthan, S. Lenzner, B.C. Hamel, S. Schweiger, H.H. Ropers, Mutations in the polyglutamine binding protein 1 gene cause X-linked mental retardation, Nat. Genet. 35 (2003) 313–315.
[4] C. Lenski, F. Abidi, A. Meindl, A. Gibson, M. Platzer, R. Frank Kooy, H.A. Lubs, R.E. Stevenson, J. Ramser, C.E. Schwartz, Novel truncating mutations in the polyglutamine tract binding protein 1 gene (PQBP1) cause Renpenning syndrome and X-linked mental retardation in another family with microcephaly, Am. J. Hum. Genet. 74 (2004) 777–780.
[5] M. Waragai, C.H. Lammers, S. Takeuchi, I. Imafuku, Y. Udagawa, I. Kanazawa, M. Kawabata, M.M. Mouradian, H. Okazawa, PQBP-1, a novel polyglutamine tract-binding protein, inhibits transcription activation by Brn-2 and affects cell survival, Hum. Mol. Genet. 8 (1999) 977–987.
[6] H. Okazawa, M. Sudol, T. Rich, PQBP-1 (Np/PQ): a polyglutamine tract-binding and nuclear inclusion-forming protein, Brain Res. Bull. 56 (2001) 273–280.
[7] H. Okazawa, T. Rich, A. Chang, X. Lin, M. Waragai, M. Kajikawa, Y. Enokido, A. Komuro, S. Kato, M. Shibata, H. Hatanaka, M.M. Mouradian, M. Sudol, I. Kanazawa, Interaction between mutant ataxin-1 and PQBP-1 affects transcription and cell death, Neuron 34 (2002) 701–713.
[8] Y. Qi, M. Hoshino, Y. Wada, S. Marubuchi, N. Yoshimura, I. Kanazawa, K. Shinomiya, H. Okazawa, PQBP-1 is expressed predominantly in the central nervous system during development, Eur. J. NeuroSci. 22 (2005) 1277–1286.
[9] H. Ito, N. Yoshimura, M. Kurosawa, S. Ishii, N. Nukina, H. Okazawa, Knock-down of PQBP1 impairs anxiety-related cognition in mouse, Hum. Mol. Genet. 18 (2009) 4239–4254.
[10] M. Waragai, E. Junn, M. Kajikawa, S. Takeuchi, I. Kanazawa, M. Shibata, M.M. Mouradian, H. Okazawa, PQBP-1/Npw38, a nuclear protein binding to the polyglutamine tract, interacts with U5-15kD/dim1p via the carboxyl-terminal domain, Biochem. Biophys. Res. Commun. 273 (2000) 592–595.
[11] Y. Zhang, T. Lindblom, A. Chang, M. Sudol, A.E. Sluder, E.A. Golemis, Evidence that dim1 associates with proteins involved in pre-mRNA splicing, and delineation of residues essential for dim1 interactions with hnRNP F and Npw38/PQBP-1, Gene 257 (2000) 33–43.
[12] M. Takahashi, M. Mizuguchi, H. Shinoda, T. Aizawa, M. Demura, H. Okazawa, K. Kawano, Polyglutamine tract binding protein-1 is an intrinsically unstructured protein, Biochim. Biophys. Acta 1794 (2009) 936–943.
[13] Y.Z. Zhang, H. Cheng, K.L. Gould, E.A. Golemis, H. Roder, Structure, stability, and function of hDim1 investigated by NMR, circular dichroism, and mutational analysis, Biochemistry 42 (2003) 9609–9618.
[14] T. Jin, F. Guo, Y. Wang, Y.Z. Zhang, Identification of human dim1 as a peptidase with autocleavage activity, Chem. Biol. Drug Des. 68 (2006) 266–272.
[15] F. Delaglio, S. Grzesiek, G.W. Vuister, G. Zhu, J. Pfeifer, A. Bax, NMRPipe: a multidimensional spectral processing system based on UNIX pipes, J. Biomol. NMR 6 (1995) 277–293.
[16] B.A. Johnson, Using NMR View to visualize and analyze the NMR spectra of macromolecules, Methods Mol. Biol. 278 (2004) 313–352.
[17] K.W. Lo, S. Naisbitt, J.S. Fan, M. Sheng, M. Zhang, The 8-kDa dynein light chain binds to its targets via a conserved (K/R)XTQT motif, J. Biol. Chem. 276 (2001) 14059–14066.
[18] K. Reuter, S. Nottrott, P. Fabrizio, R. Lührmann, R. Ficner, Identification, characterization and crystal structure analysis of the human spliceosomal U5 snRNP-specific 15 kD protein, J. Mol. Biol. 294 (1999) 515–525.
[19] J. Zamoon, F. Nitu, C. Karim, D.D. Thomas, G. Veglia, Mapping the interaction surface of a membrane protein: unveiling the conformational switch of phospholamban in calcium pump regulation, Proc. Natl. Acad. Sci. U. S. A. 102 (2005) 4747–4752.
[20] A.K. Sharma, G.P. Zhou, J. Kupferman, H.K. Surks, E.N. Christensen, J.J. Chou, M.E. Mendelsohn, A.C. Rigby, Probing the interaction between the coiled coil leucine zipper of cGMP-dependent protein kinase Ialpha and the C terminus of the myosin binding subunit of the myosin light chain phosphatase, J. Biol. Chem. 283 (2008) 32860–32869.

[21] M. Sette, P. Van Tilborg, R. Spurio, R. Kaptein, M. Paci, C.O. Gualerzi, R. Boelens, The structure of the translational initiation factor IF1 from *E. coli* contains an oligomer-binding motif, EMBO J. 16 (1997) 1436–1443.
[22] H. Matsuo, K.J. Walters, K. Teruya, T. Tanaka, G.T. Gassner, S.J. Lippard, Y. Kyogoku, G. Wagner, Identification by NMR spectroscopy of residues at contact surfaces in large, slowly exchanging macromolecular complexes, J. Am. Chem. Soc. 121 (1999) 9903–9904.
[23] H.J. Dyson, P.E. Wright, Unfolded proteins and protein folding studied by NMR, Chem. Rev. 104 (2004) 3607–3622.
[24] P.E. Wright, H.J. Dyson, Intrinsically unstructured proteins: re-assessing the protein structure–function paradigm, J. Mol. Biol. 293 (1999) 321–331.
[25] A.K. Dunker, C.J. Brown, J.D. Lawson, L.M. Iakoucheva, Z. Obradović, Intrinsic disorder and protein function, Biochemistry 41 (2002) 6573–6582.
[26] P. Tompa, Intrinsically unstructured proteins, Trends Biochem. Sci. 27 (2002) 527–533.
[27] P. Tompa, M. Fuxreiter, C.J. Oldfield, I. Simon, A.K. Dunker, V.N. Uversky, Close encounters of the third kind: disordered domains and the interactions of proteins, Bioessays 31 (2009) 328–335.
[28] J.J. Ward, J.S. Sodhi, L.J. McGuffin, B.F. Buxton, D.T. Jones, Prediction and functional analysis of native disorder in proteins from the three kingdoms of life, J. Mol. Biol. 337 (2004) 635–645.
[29] E. Hazy, P. Tompa, Limitations of induced folding in molecular recognition by intrinsically disordered proteins, Chemphyschem 10 (2009) 1415–1419.
[30] H.J. Dyson, P.E. Wright, Coupling of folding and binding for unstructured proteins, Curr. Opin. Struct. Biol. 12 (2002) 54–60.
[31] C.M. Fletcher, A.M. McGuire, A.C. Gingras, H. Li, H. Matsuo, N. Sonenberg, G. Wagner, 4E binding proteins inhibit the translation factor eIF4E without folded structure, Biochemistry 37 (1998) 9–15.
[32] A.B. Sigalov, W.M. Kim, M. Saline, L.J. Stern, The intrinsically disordered cytoplasmic domain of the T cell receptor zeta chain binds to the nef protein of simian immunodeficiency virus without a disorder-to-order transition, Biochemistry 47 (2008) 12942–12944.
[33] T. Clackson, J.A. Wells, A hot spot of binding energy in a hormone-receptor interface, Science 267 (1995) 383–386.
[34] A.M. de Vos, M. Ultsch, A.A. Kossiakoff, Human growth hormone and extracellular domain of its receptor: crystal structure of the complex, Science 255 (1992) 306–312.
[35] T.K. Nielsen, S. Liu, R. Lührmann, R. Ficner, Structural basis for the bifunctionality of the U5 snRNP 52K protein (CD2BP2), J. Mol. Biol. 369 (2007) 902–908.
[36] B. Laggerbauer, S. Liu, E. Makarov, H.P. Vornlocher, O. Makarova, D. Ingelfinger, T. Achsel, R. Lührmann, The human U5 snRNP 52K protein (CD2BP2) interacts with U5-102K (hPrp6), a U4/U6.U5 tri-snRNP bridging protein, but dissociates upon tri-snRNP formation, RNA 11 (2005) 598–608.
[37] O.V. Makarova, E.M. Makarov, H. Urlaub, C.L. Will, M. Gentzel, M. Wilm, R. Lührmann, A subset of human 35S U5 proteins, including Prp19, function prior to catalytic step 1 of splicing, EMBO J. 23 (2004) 2381–2391.
[38] F. Simeoni, G. Divita, The Dim protein family: from structure to splicing, Cell. Mol. Life Sci. 64 (2007) 2079–2089.
[39] L.D. Berry, K.L. Gould, Fission yeast dim1(+) encodes a functionally conserved polypeptide essential for mitosis, J. Cell Biol. 137 (1997) 1337–1354.
[40] F. Simeoni, A. Arvai, P. Bello, C. Gondeau, K.P. Hopfner, P. Neyroz, F. Heitz, J. Tainer, G. Divita, Biochemical characterization and crystal structure of a Dim1 family associated protein: Dim2, Biochemistry 44 (2005) 11997–12008.